Molecular collisions in the interstellar medium

David Flower

2

Interstellar shocks and chemistry

2.1 Introduction

Considerable effort has been directed at studying the formation of molecular species in the ambient intestellar medium. By 'ambient' is to be understood the cold gas whose equilibrium temperature is determined by the balance of heating through the action of cosmic or X-rays and of the interstellar background radiation field at wavelengths $\lambda > 91.2$ nm. Models have been made of both diffuse and dense clouds, using both chemical equilibrium and time–dependent codes. There have been many publications in this area; they all owe much to the pioneering studies of Herbst & Klemperer [12] and Black & Dalgarno [21].

In the ambient medium, the kinetic temperature of the gas is low ($T \lesssim 100$ K) and even mildly endothermic processes, such as the important charge exchange reaction

$$H^+ + O \rightarrow H + O^+ - 227\ K \tag{2.1}$$

are effectively inhibited. The gas–phase chemistry of the ambient medium is dominated by reactions with no endothermicity and no reaction barrier.

Observations of molecular clouds have established beyond reasonable doubt that shocks propagate within them. Hyperthermal molecular line widths and emission from highly excited states of molecules, particularly H_2 and CO, indicate that shock wave heating is occurring in the Orion molecular cloud, for example. shocks, driven by turbulent motions in molecular clouds and the expansion of compact H II regions, or by the jets of matter associated with the formation of proto-stars, are undoubtedly a common phenomenon.

Whilst passage through a shock wave is a mechanism for producing vibrationally excited H_2 molecules [22], [23], [24], calculations show that, for shock speeds $u_s \gtrsim 20$ km s^{-1}, the H_2 would be dissociated by thermal collisions on passing through the shock front. As line width measurements indicated shock speeds much in excess of 20 km s^{-1} (e.g. [25]), there appeared to be an inconsistency in the shock–excitation hypothesis.

In early work on hydromagnetic shock waves in the interstellar medium [26], the ionized and neutral fluids were assumed to be fully coupled. In this case, the action of the magnetic field (on the ionized gas) is simultaneously transmitted to the neutral gas. Field et al. recognized that, if the degree of ionization is low, appreciable decoupling of the flows of the ionized and the neutral fluids might ensue. The magnetic field may be considered to be 'frozen' in the ionized fluid, which is electrically

conducting. When the magnetic field has a component perpendicular to the flow direction, the compression of the ionized gas is accompanied by the compression of the magnetic field; but the effects of this compression are felt by the neutrals, via collisions with the ions, only after a delay. Differences develop in the flow speeds of the charged and neutral fluids, a phenomenon which is termed "ion–neutral drift", from the viewpoint of the fluids, or "ambipolar diffusion", from the viewpoint of the magnetic field (which diffuses through the neutrals, together with the ions).

Effects associated with the partial decoupling of the charged and neutral fluids were subsequently investigated by Mullan [27]. As a consequence of ambipolar diffusion, the neutral fluid is compressed and heated in advance of the shock discontinuity. This heating mechanism was incorporated, in an approximate manner, into the shock model of Hollenbach & McKee [28], but it was not until the work of Draine [29] that a quantitative model of such magnetohydrodynamical (MHD) shock waves became available. The model of Draine, like its predecessors, assumed that steady state had been attained; only recently have time–dependent models – which describe the temporal evolution as well as the spatial structure of shock waves – found their way into the literature [30], [31], [32], [33].

As a result of shock wave heating, chemical reactions which are endothermic, or which present reaction barriers attaining a few tenths of an eV, become significant. The requisite energy derives from the motion of the shock wave (i.e. from the 'piston' which drives it) and is transmitted to the gas in the form of thermal energy and, in MHD shocks, through the ion–neutral drift. Thus, reactions such as

$$C^+ + H_2 \rightarrow CH^+ + H - 4640 \text{ K} \tag{2.2}$$

and

$$O + H_2 \rightarrow OH + H \tag{2.3}$$

which has a barrier of 2980 K, are unimportant in the ambient medium but assume significance in regions which have undergone shock heating.

Just as the shock structure is important in determining the chemistry of the medium, so the chemistry is important to the structure of the shock wave. Chemical reactions affect directly the degree of ionization of the medium and hence the interaction with the magnetic field. Furthermore, chemical reactions influence the abundances of the atomic and molecular species which cool the gas, principally through the collisional excitation of rovibrational (Chapters 4 and 5) and fine structure (Chapter 6) transitions. The dynamical and chemical conservation equations are interdependent and must be solved in parallel. So too must the equations for the population densities of the rovibrational levels of the H_2 molecule, which is the main coolant of shocked molecular gas. There is a delay in in the response of the level populations to changes in the density and the kinetic temperature of the gas; this delay is taken into account only when the equations for the level populations are integrated *in parallel* with the MHD and chemical conservation equations, to which we now turn.

2.2 The MHD conservation equations

The quantities with which we shall be concerned are the numbers of particles, their mass, momentum and energy. It has already been mentioned that the ionized

and neutral fluids can develop different flow velocities; their temperatures may also differ. Furthermore, the temperatures of the ions and the electrons at any given point in the flow may not be equal. The development of differences in the velocities of the positively and negatively charged fluids is resisted by large electrical forces; these ensure that the velocities and the number densities of the positive and negative particles are effectively equal everywhere.

2.2.1 The equations in one dimension

In the analysis which follows, it will be assumed that a stationary state has been attained, in which case $\partial/\partial t = 0$. The total time derivative may then be written as

$$\frac{\mathrm{d}}{\mathrm{d}t} = \frac{\partial}{\partial t} + \mathbf{u}\cdot\bigtriangledown = \mathbf{u}\cdot\bigtriangledown \tag{2.4}$$

where $\mathbf{u}$ is the flow velocity and $\bigtriangledown = \hat{\mathbf{i}}\partial/\partial x + \hat{\mathbf{j}}\partial/\partial y + \hat{\mathbf{k}}\partial/\partial z$ is the gradient operator. If the flow is plane–parallel in the z-direction, then $\bigtriangledown = \hat{\mathbf{k}}\partial/\partial z$ and

$$\frac{\mathrm{d}}{\mathrm{d}t} = u\frac{\mathrm{d}}{\mathrm{d}z} \tag{2.5}$$

By making these assumptions, we exclude the possibility of studying rigorously both the temporal evolution of the shock wave and its structure in more than one spatial dimension; but we simplify considerably the numerical aspects of the problem, which reduces to solving coupled *ordinary* (rather than partial) differential equations.

Subject to the assumptions above, the equation for the number density of neutral particles states that

$$\frac{\mathrm{d}}{\mathrm{d}z}(\rho_{\mathrm{n}} u_{\mathrm{n}}/\mu_{\mathrm{n}}) = \mathcal{N}_{\mathrm{n}} \tag{2.6}$$

where ρ_{n} is the mass density of the neutrals at the point z, μ_{n} their mean molecular weight, and u_{n} is their flow speed in the z-direction.The 'source' term on the right hand side of equation (2.6) is the rate of creation (or destruction, if negative) of neutral particles per unit volume through recombination and ionization processes. For example, the formation of molecular from atomic hydrogen results in a net reduction in the number of neutral particles ($\mathcal{N}_{\mathrm{n}} < 0$).

An analogous equation holds for the positively (and the negatively) charged fluid,

$$\frac{\mathrm{d}}{\mathrm{d}z}(\rho_{+} u_{+}/\mu_{+}) = \mathcal{N}_{+} \tag{2.7}$$

The positively charged fluid, denoted by '+', comprises the positive ions and positively charged grains. In general, $\mathcal{N}_{\mathrm{n}} \neq -\mathcal{N}_{+}$: dissociative recombination processes, for example,

$$\mathrm{CH}^{+} + \mathrm{e}^{-} \rightarrow \mathrm{C} + \mathrm{H} \tag{2.8}$$

result in the destruction of *one* ion but create *two* neutrals.

The equation of mass conservation for the neutrals may be written

$$\frac{\mathrm{d}}{\mathrm{d}z}(\rho_{\mathrm{n}} u_{\mathrm{n}}) = \mathcal{S}_{\mathrm{n}} \tag{2.9}$$

where $\mathcal{S}_{\rm n}$ denotes the rate per unit volume at which neutral mass is created or destroyed. The corresponding equation for the positively charged fluid is

$$\frac{\mathrm{d}}{\mathrm{d}z}(\rho_+ u_+) = \mathcal{S}_+ \tag{2.10}$$

As neutral mass may be created only through the destruction of charged mass, by recombination of positively and negatively charged particles, $\mathcal{S}_+ + \mathcal{S}_- = -\mathcal{S}_{\rm n}$, where the subscript '$-$' refers to the negatively charged fluid, which comprises the electrons, negative ions and the negatively charged grains. When the negatively charged particle in the recombination reaction is an electron, which is most frequently the case, $\mathcal{S}_-$ is negligible.

Momentum must also be conserved; for the neutral fluid, the equation of momentum conservation takes the form

$$\frac{\mathrm{d}}{\mathrm{d}z}\left(\rho_{\rm n} u_{\rm n}^2 + \frac{\rho_{\rm n} k_{\rm B} T_{\rm n}}{\mu_{\rm n}}\right) = \mathcal{A}_{\rm n} \tag{2.11}$$

where $T_{\rm n}$ is the temperature of the neutral fluid at the point z, and $\mathcal{A}_{\rm n}$ determines the rate at which momentum is being gained or lost by unit volume of the neutral gas. Momentum transfer occurs principally in collisions of the neutrals with ions and with charged grains. As the positively and the negatively charged particles have the same number density and the same flow speed, their combined equation of momentum conservation may be written

$$\frac{\mathrm{d}}{\mathrm{d}z}\left[(\rho_+ + \rho_-)u_+^2 + \frac{\rho_+ k_{\rm B}(T_+ + T_-)}{\mu_+} + \frac{B^2}{8\pi}\right] = -\mathcal{A}_{\rm n} \tag{2.12}$$

where we have used the fact that $\rho_+/\mu_+ = \rho_-/\mu_-$, owing to the overall charge neutrality. In equation (2.12), B is the component of the magnetic field perpendicular to the z-direction, and $B^2/(8\pi)$ is the magnetic pressure term. The magnetic field acts directly on the charged fluid, which communicates its effects to the neutral fluid through collision processes. If the magnetic field is assumed to be 'frozen' into the charged fluid, the condition

$$B u_+ = B_0 u_s \tag{2.13}$$

is satisfied; B_0 is the value of the magnetic field strength upstream of the shock wave, in the 'preshock' gas, and u_s is the shock speed. In the reference frame of the shock wave, in which the conservation equations are formulated, the initial ('upstream' or 'preshock') flow speeds of the neutral and charged fluids are both equal to the shock speed. Taking the flow to be in the positive z-direction implies that the shock wave is propagating in the negative z-direction.

The condition of energy conservation, applied to the neutral fluid, yields

$$\frac{\mathrm{d}}{\mathrm{d}z}\left[\frac{\rho_{\rm n} u_{\rm n}^3}{2} + \frac{5\rho_{\rm n} u_{\rm n} k_{\rm B} T_{\rm n}}{2\mu_{\rm n}} + \frac{\rho_{\rm n} u_{\rm n} U_{\rm n}}{\mu_{\rm n}}\right] = \mathcal{B}_{\rm n} \tag{2.14}$$

where $U_{\rm n}$ denotes the mean internal energy per neutral particle, and $\mathcal{B}_{\rm n}$ is the rate of gain (or loss, if negative) of energy per unit volume of the neutral fluid. The internal energy consists essentially of the rovibrational excitation energy of the H_2 molecule,

whose excited state population densities can become appreciable as the temperature and the density increase, owing to the passage of the shock wave.

In order to discriminate between the temperatures of the positively and negatively charged fluids, it is necessary to separate their energy conservation relations. Draine [34] derived these equations for the case of a MHD shock wave. However, the difference between T_+ and T_- is difficult to evaluate accurately, and it has only a minor influence on the dynamical and chemical structure of the shock wave, in general. Accordingly, we consider the combined equation of energy conservation of the (positively and negatively) charged fluid, which takes the form

$$\frac{\mathrm{d}}{\mathrm{d}z}\left[(\rho_+ + \frac{\rho_-)u_+^3}{2} + \frac{5\rho_+ u_+ k_\mathrm{B}(T_+ + T_-)}{2\mu_+} + \frac{u_+ B^2}{4\pi}\right]$$
$$= \mathcal{B}_+ + \mathcal{B}_- \tag{2.15}$$

where $(\mathcal{B}_+ + \mathcal{B}_-)$ is the rate of energy gain per unit volume of the charged fluid.

2.2.2 The role of the magnetic field

We have already seen that the selective action of the magnetic field on the charged particles can give rise to different flow speeds for the charged and the neutral fluids. Consider first the neutral fluid. If a sonic point occurs in the flow, at the point where

$$u_\mathrm{n}^2 = \frac{5k_\mathrm{B}T_\mathrm{n}}{3\mu_\mathrm{n}} \equiv c_\mathrm{s}^2 \tag{2.16}$$

and c_s is the adiabatic sound speed, then the neutral flow becomes discontinuous and a shock occurs. In fact, this shock 'discontinuity' has a finite thickness, owing to viscous forces, which is of the same order as the length scale which characterizes elastic collisions between the neutral particles.

It is possible to integrate the conservation equations through the shock 'discontinuity' by introducing *artificial viscosity* terms [35]. Providing the transition from the pre- to the post-shock gas occurs adiabatically, i.e. processes of energy transfer (notably radiative losses) are negligible, integration of the conservation equations through the 'discontinuity' automatically satisfies the Rankine–Hugoniot relations. The latter specify the compression ratio and the temperature ratio across the shock front, in the limit in which the shock front may be treated as a discontinuity; the Rankine–Hugoniot relations are derived in Section 2.3.1 below.

Similarly, a discontinuity occurs in the flow of the charged fluid at the point at which

$$u_+^2 = \frac{5k_\mathrm{B}(T_+ + T_-)}{3(\mu_+ + \mu_-)} + \frac{B^2}{4\pi(\rho_+ + \rho_-)} \equiv c_\mathrm{m}^2 \tag{2.17}$$

where c_m is the magnetosonic speed in the charged fluid. As $u_+ \leq u_s$ everywhere, in the reference frame of the shock wave, a discontinuity in the flow of the charged fluid cannot occur if

$$u_s < c_\mathrm{m}$$

a condition which is satisfied in magnetically dominated flows. It follows that flows can exist which are discontinuous in only the neutral flow variables.

In practice, modest values of the magnetic field strength are sufficient to suppress the discontinuity in the flow variables of the charged fluid when the degree of ionization of the medium is low. For example, if $u_s = 10$ km s^{-1} and the charged mass density $\rho_+ + \rho_- = 2 \times 10^{-25}$ g cm^{-3} (corresponding to C^+ ions in a medium with a total particle density of about 50 cm^{-3}), $B \approx 1$ μG is all that is required.

The region upstream of the discontinuity, in which the charged fluid has been compressed along with the magnetic field, has been termed the 'magnetic precursor' or 'acceleration zone'; the width of the precursor increases with the magnetic field strength. As the shock evolves, the discontinuity in the neutral flow moves progressively downstream and weakens, until finally the discontinuity is suppressed. Thus, for sufficiently large field strengths, the shock wave evolves from 'jump' or J–type, to J–type with a magnetic precursor, to 'continuous' or C–type [31]. To describe this evolution rigorously, a time–dependent MHD code must be used; but the evolution can be simulated by means of calculations which are not explicitly time–dependent, as will be seen below. The mass density of the charged fluid, $\rho_+ + \rho_-$, is a factor determining the magnetosonic speed and hence the width of the acceleration zone. The endothermic reaction (1.26) of C^+ ions with H_2 molecules can be initiated by ion–neutral drift in this zone, yielding CH^+. The rapid exothermic reactions

$$CH^+ + H_2 \rightarrow CH_2^+ + H \tag{2.18}$$

and

$$CH_2^+ + H_2 \rightarrow CH_3^+ + H \tag{2.19}$$

then lead to the formation of CH_2^+ and CH_3^+. The molecular ions are destroyed by dissociative recombination reactions, such as

$$CH^+ + e^- \rightarrow C + H \tag{2.20}$$

which are believed to be rapid at the relevant temperatures. The net result is the neutralization of an important part of the ionized component of the gas. This process, of partial neutralization, can occur on a distance scale which is comparable with the dimensions of the acceleration zone, resulting in a significant enhancement of the width of this zone through the increase in the magnetic field term in equation (2.17).

In diffuse clouds, the situation is rendered more complicated by photoionization processes, notably

$$C + h\nu \rightarrow C^+ + e^- \tag{2.21}$$

which restore ions to the medium and which also occur over a characteristic distance scale which is comparable with the width of the acceleration zone. However, before considering further the chemistry in shock waves, in both diffuse and dense clouds, it is appropriate to consider in more detail the 'source terms' $(\mathcal{N}, \mathcal{S}, \mathcal{A}, \mathcal{B})$ appearing in the MHD conservation equations.

2.2.3 The source terms

The 'source terms' which appear on the right hand sides of the MHD conservation equations presented above contain the micro-physics of the problem. These terms describe the interactions between the particles of the medium, including the grains, and the ways in which these interactions modify the number and mass densities, momentum and energy of the charged and neutral fluids. The principal terms will be introduced below; their hierarchy of importance depends on the context of the problem being considered. For a detailed discussion of the source terms, the reader may consult the paper of Draine [34].

Let us denote the net rate at which a particular atomic or molecular species, α, is produced per unit volume by $\mathcal{C}_\alpha$; a net destruction rate corresponds to $\mathcal{C}_\alpha < 0$. The total number of neutral particles produced per unit volume and time is

$$\mathcal{N}_{\rm n} = \sum_{\alpha_{\rm n}} \mathcal{C}_{\alpha_{\rm n}} \tag{2.22}$$

where the subscript 'n' identifies the species as being neutral. Similarly, for the positive ions

$$\mathcal{N}_{+} = \sum_{\alpha_{+}} \mathcal{C}_{\alpha_{+}} \tag{2.23}$$

As already noted, $\mathcal{N}_{+} \neq -\mathcal{N}_{\rm n}$, in general.

Creation of neutral mass proceeds at a rate per unit volume

$$\mathcal{S}_{\rm n} = \sum_{\alpha_{\rm n}} \mathcal{C}_{\alpha_{\rm n}} m_{\alpha_{\rm n}} \tag{2.24}$$

where $m_{\alpha_{\rm n}}$ is the mass of the neutral species $\alpha_{\rm n}$; the corresponding expression for the positive ions is

$$\mathcal{S}_{+} = \sum_{\alpha_{+}} \mathcal{C}_{\alpha_{+}} m_{\alpha_{+}} \tag{2.25}$$

In this case, $\mathcal{S}_{+} + \mathcal{S}_{-} = -\mathcal{S}_{\rm n}$ must be satisfied.

Momentum is transferred between the charged and the neutral fluids through ion–neutral reactions and elastic scattering. Denoting a particular ion–neutral reaction by β, we may write

$$\mathcal{C}_\alpha = \sum_{\beta} \mathcal{C}_{\alpha\beta} \tag{2.26}$$

and the associated rate of momentum transfer from the charged to the neutral fluid is

$$\mathcal{A}_{\rm n}^{\rm (i)} = \sum_{\alpha_{\rm n}\beta} \left[\sum_{\mathcal{C}_{\alpha_{\rm n}\beta}>0} \mathcal{C}_{\alpha_{\rm n}\beta} m_{\alpha_{\rm n}} u_\beta({\rm CM}) + \sum_{\mathcal{C}_{\alpha_{\rm n}\beta}<0} \mathcal{C}_{\alpha_{\rm n}\beta} {\rm m}_{\alpha_{\rm n}} {\rm u_n} \right] \tag{2.27}$$

where the centre–of–mass collision velocity is given by

$$u_\beta({\rm CM}) = \frac{m_{\rm i} u_{\pm} + m_{\rm n} u_{\rm n}}{m_{\rm i} + m_{\rm n}} \tag{2.28}$$

where $m_{\rm i}$ is the mass of a (positive or negative) ion and $m_{\rm n}$ is the mass of the neutral. Equation (2.27) expresses the fact that, when a neutral is a product and hence $\mathcal{C}_{\alpha_{\rm n}\beta} > 0$, it is created at the centre–of–mass velocity of the reaction β. On the other hand, when a neutral is a reactant ($\mathcal{C}_{\alpha_{\rm n}\beta} < 0$), it is removed whilst moving with the velocity of the neutral fluid, $u_{\rm n}$.

Osterbrock [36] derived an expression for the cross section for momentum transfer in a collision between a charged and a neutral particle from considerations of the long–range charge–induced dipole interaction between the colliding pair; the expression which Osterbrock derived is

$$\sigma_{in} = 2.41\pi \left[\frac{e^2 \alpha_{\rm n}}{(m_{\rm in} v_{\rm in}^2} \right]^{\frac{1}{2}} \tag{2.29}$$

where e is the electron charge, $\alpha_{\rm n}$ is the polarizability of the neutral, $m_{\rm in} = m_{\rm i} m_{\rm n}/(m_{\rm i} + m_{\rm n})$ is the reduced mass of the ion-neutral pair, and $v_{\rm in}$ is the relative collision speed. The expression (2.29) exceeds by 20 per cent the 'Langevin' cross section (cf. Chapter 8). Equation (2.29) has been shown to be valid at low collision speeds but to underestimate the momentum transfer at high collision speeds [37]. The polarizabilities of the principal constituents of the neutral fluid are: atomic hydrogen, $\alpha_{\rm H} = 4.5\ a_0^3$; molecular hydrogen, $\alpha_{\rm H_2} = 5.2\ a_0^3$; and helium, $\alpha_{\rm He} = 1.4\ a_0^3$. The polarizabilities of H and H_2 are similar in magnitude and substantially larger than that of He.

The rate of transfer of momentum to the neutral fluid, owing to elastic scattering on the ions, is given by

$$\mathcal{A}_{\rm n}^{\rm (ii)} = \frac{\rho_{\rm n}\rho_{\rm i}}{\mu_{\rm n} + \mu_{\rm i}} \langle \sigma v \rangle_{\rm in} (u_{\rm i} - u_{\rm n}) \tag{2.30}$$

where

$$\langle \sigma v \rangle_{\rm in} = 2.41\pi \left(\frac{e^2 \alpha_{\rm n}}{\mu_{\rm in}} \right)^{\frac{1}{2}} \tag{2.31}$$

is the corresponding rate coefficient; $\mu_{\rm in} = \mu_{\rm i}\mu_{\rm n}/(\mu_{\rm i} + \mu_{\rm n})$ is the reduced mass, evaluated using the mean molecular weights of the ionized and neutral fluids.

Momentum transfer between the neutral gas and charged grains is important in dense clouds, where the degree of ionization of the gas is low. In this case, the cross section may be taken approximately equal to the the geometrical cross section of the grain, $\pi a_{\rm g}^2$, where $a_{\rm g}$ is the grain radius. (There is a correction to the geometrical cross section, significant at low collision speeds, arising from the polarization of the neutral by the charged grain [38]). As the the collision speed is, to a good approximation, equal to the ion-neutral drift speed, $|u_{\rm i} - u_{\rm n}|$, and $\mu_{\rm g} >> \mu_{\rm n}$, the rate of momentum transfer between the neutral gas and the charged grains (in dense clouds, most of the grains have a single negative charge) is

$$\mathcal{A}_{\rm n}^{\rm (iii)} = \rho_{\rm n} n_{\rm g} \pi a_{\rm g}^2 |u_{\rm i} - u_{\rm n}| (u_{\rm i} - u_{\rm n}) \tag{2.32}$$

The total rate of momentum transfer is $\mathcal{A}_{\rm n} = \mathcal{A}_{\rm n}^{\rm (i)} + \mathcal{A}_{\rm n}^{\rm (ii)} + \mathcal{A}_{\rm n}^{\rm (iii)}$.

Various physical processes lead to energy exchange between the charged and the neutral fluids. Chemical reactions are responsible for kinetic energy transfer from the charged to the neutral fluid, at a rate per unit volume

$$\mathcal{B}_{\rm n}^{\rm (i)} = \sum_{\alpha_{\rm n}\beta} \left[\sum_{\mathcal{C}_{\alpha_{\rm n}\beta}>0} \mathcal{C}_{\alpha_{\rm n}\beta} \frac{1}{2} m_{\alpha_{\rm n}} u_\beta^2({\rm CM}) + \sum_{\mathcal{C}_{\alpha_{\rm n}\beta}<0} \mathcal{C}_{\alpha_{\rm n}\beta} \frac{1}{2} {\rm m}_{\alpha_{\rm n}} {\rm u}_{\rm n}^2 \right] \tag{2.33}$$

An analogous expression holds for transfer of kinetic energy from the neutral to the charged fluid; the kinetic energy of the electrons may be neglected, in comparison with that of the ions.

When considering heat transfer between fluids, a distinction has to be made once again between formation ($\mathcal{C}_{\alpha_{\rm n}\beta} > 0$) and destruction ($\mathcal{C}_{\alpha_{\rm n}\beta} < 0$) processes. When an ion and an electron at temperatures T_+ and T_-, respectively, dissociatively recombine to form two neutrals, as in the reaction

$$\mathrm{CH^+ + e^- \rightarrow C + H} \tag{2.34}$$

an amount of heat $3k_{\rm B}(T_+ + T_-)/2$ is transferred to the neutral fluid. On the other hand, an amount of heat $3k_{\rm B}T_{\rm n}/2$ is lost by the neutral fluid through photoionization , as in

$$\mathrm{C} + h\nu \rightarrow \mathrm{C^+ + e^-} \tag{2.35}$$

The net rate of thermal energy transfer to the neutral fluid is

$$\mathcal{B}_{\rm n}^{\rm (ii)} = \sum_{\alpha_{\rm n}\beta} \left[\sum_{\mathcal{C}_{\alpha_{\rm n}\beta}>0} \mathcal{C}_{\alpha_{\rm n}\beta} \frac{3}{2} k_{\rm B} \frac{T_+ + T_-}{2} + \sum_{\mathcal{C}_{\alpha_{\rm n}\beta}<0} \mathcal{C}_{\alpha_{\rm n}\beta} \frac{3}{2} k_{\rm B} \frac{T_{\rm n}}{2} \right] \tag{2.36}$$

Dissociative recombination and photoionization are the most rapid and important processes determining the degree of ionization in shocks propagating in diffuse interstellar clouds. In the interiors of dense clouds, the degree of ionization is lower, owing to the absence of ionizing photons, which are absorbed and scattered by dust in the outer layers; cosmic ray ionization takes over but is a slow process.

When photoionization does occur, the corresponding heating rate is given by

$$\mathcal{B}_-^{\rm (iii)} = \sum_\alpha n_\alpha \int_{\nu_\alpha}^{\nu_{\rm H}} \frac{4\pi J_\nu}{h\nu} a_\nu(\alpha)(h\nu - h\nu_\alpha)\ {\rm d}\nu \tag{2.37}$$

where J_ν is the mean radiation intensity at frequency ν, $a_\nu(\alpha)$ is the frequency–dependent photoionization cross section of species α, and ν_α is the photoionization threshold frequency. The integral extends to the Lyman limit in atomic hydrogen, $h\nu = 13.598$ eV; photons of higher energy tend to be absorbed (by atomic hydrogen) in the immediate vicinities of the sources of the ultraviolet radiation.

Chemical reactions also affect the thermal balance of the medium by virtue of their energy defects, ΔE. The corresponding rate of heating of the neutral fluid is

$$\mathcal{B}_{\rm n}^{\rm (iv)} = \sum_{\alpha_{\rm n}\beta} \sum_{\mathcal{C}_{\alpha_{\rm n}\beta}>0} \mathcal{C}_{\alpha_{\rm n}\beta} \frac{M_\beta - m_{\alpha_{\rm n}}}{M_\beta} \Delta E_\beta \tag{2.38}$$

where M_β is the total mass of the products of reaction β, including $m_{\alpha_{\rm n}}$. The factor $(M_\beta - m_{\alpha_{\rm n}})/M_\beta$ determines the partition of energy amongst the reaction products, with the lighter products carrying off more of the energy, ΔE_β, released in the reaction.

Elastic scatering of the neutrals on the ions results in the exchange of energy between the fluids. The neutral fluid is heated through this process at a rate given by

$$\mathcal{B}_{\rm n}^{(\rm v)} = \frac{\rho_{\rm n}\rho_{\rm i}}{\mu_{\rm n}\mu_{\rm i}}\langle\sigma v\rangle_{\rm in}\frac{2\mu_{\rm n}\mu_{\rm i}}{(\mu_{\rm n}+\mu_{\rm i})^2}[\frac{3}{2}k_{\rm B}(T_{\rm i}-T_{\rm n})+\frac{1}{2}(u_{\rm i}-u_{\rm n})(\mu_{\rm i}u_{\rm i}+\mu_{\rm n}u_{\rm n})] \quad (2.39)$$

where the rate coefficient for ion-neutral elastic scattering, $\langle\sigma v\rangle_{\rm in}$, is given by equation (2.31) above. Inspection of equation (2.39) shows that $\mathcal{B}_{\rm i}^{(\rm v)} = -\mathcal{B}_{\rm n}^{(\rm v)}$. The corresponding rate of energy transfer from the charged grains to the neutral fluid is

$$\mathcal{B}_{\rm n}^{(\rm vi)} = \rho_{\rm n} n_{\rm g}\pi a_{\rm g}^2|u_{\rm i}-u_{\rm n}|(u_{\rm i}-u_{\rm n})u_{\rm i} \quad (2.40)$$

where we assume $\mu_{\rm g} >> \mu_{\rm n}$.

Collisional excitation, followed by radiative decay at an optically thin wavelength, is an important source of energy loss from the gas and must be taken into account. Particularly significant is the collisional excitation of rovibrational transitions in molecules and of fine structure transitions in atoms and ions, as discussed in Chapters 4-6. The rates of cooling processes are proportional to the number densities of the coolants, which depend in turn on the chemical reactions occurring within the shocked gas.

In shocks which give rise to appreciable collisional dissociation of molecular hydrogen, the reformation of H_2 in the cooling flow of the shock wave represents a significant heating process. Molecular hydrogen forms on grains, and the H_2 molecules are returned to the gas phase with a finite amount of translational energy; this is subsequently converted to heat, through elastic collisions with the other constituents of the gas. The rate of heating is proportional to the rate of formation of H_2 and to the translational energy of the molecule as it leaves the grain. The total energy released when a molecule of hydrogen forms is 4.48 eV, the molecular binding energy. It is often assumed that this energy is partitioned, in equal fractions of $\frac{1}{3}$, as internal (rovibrational) and translational energies of the molecule, and with $\frac{1}{3}$ being recovered by the grain in phonon excitation. Whether this assumption is correct remains to be established, probably by means of experiments in the laboratory.

2.3 The structure of interstellar shock waves

In the previous Section, we introduced the MHD conservation equations applicable to one–dimensional, steady–state, multi–fluid flows; these equations enable the structure of C–type shock waves to be calculated. However, shock waves in the interstellar medium are not necessarily, perhaps not normally, of C–type. When a shock wave is produced, for example in a collision between interstellar clouds at supersonic relative speed, the shock wave is initially of J–type. Depending on the shock speed and the magnetic field strength, this J–type shock wave may develop a magnetic precursor and ultimately become C–type.

The shock speed, u_s, is an important parameter. The kinetic energy flux associated with the shock wave, $\frac{1}{2}\rho u_s^3$, increases rapidly with u_s. Some of this energy is used to heat the gas, at the shock discontinuity. When the temperature, T, exceeds a few thousand degrees, molecular hydrogen begins to be collisionally dissociated. Because H_2 is a major coolant, its destruction leads to a further increase in T. Ultimately,

the adiabatic sound speed, $c_{\rm s} = (\gamma k_{\rm B} T/\mu)^{\frac{1}{2}}$, where γ is the ratio of specific heats at constant pressure and volume, approaches the flow speed and a discontinuity occurs in the flow.

From the conservation relations presented in the previous Section, the equations which are applicable to the 'discontinuity' in a J–type shock wave, and to the cooling flow behind the discontinuity, may be derived. As we have already noted, the so–called 'discontinuity' has a finite width, owing to the effects of viscosity and thermal conduction, which are characterized by length scales comparable with the mean free path for elastic scattering. The process of elastic scattering tends to equalize the values of parameters, such as u and T, associated with the flows of the various fluids. Accordingly, we shall assume single–fluid flow in what follows; but we note that this assumption is not valid for the grains, particularly the more massive grains, which have large inertia.

The conservation equations for single–fluid flow are obtained by adding the equations derived in the previous Section for multi–fluid flow, i.e. for the neutral, positively and negatively charged fluids. The sums of the source terms appearing on the right hand sides of the resulting equations of conservation of mass and momentum are identically zero. However, the number density and the energy of the flow are not conserved, in general. The number density can vary because of reactions, such as the collisional dissociation of H_2

$$\mathrm{H} + \mathrm{H}_2 \rightarrow \mathrm{H} + \mathrm{H} + \mathrm{H} \tag{2.41}$$

in which there are two reactants but three products. Energy is lost from the flow in the form of radiation, as already mentioned. Thus, the conservation equations may be written in the form

$$\frac{\mathrm{d}}{\mathrm{d}z}\left(\frac{\rho u}{\mu}\right) = \mathcal{N} \tag{2.42}$$

$$\frac{\mathrm{d}}{\mathrm{d}z}(\rho u) = 0 \tag{2.43}$$

$$\frac{\mathrm{d}}{\mathrm{d}z}\left[\rho u^2 + \frac{\rho k_{\rm B} T}{\mu} + \frac{B^2}{8\pi}\right] = 0 \tag{2.44}$$

and

$$\frac{\mathrm{d}}{\mathrm{d}z}\left[\frac{\rho u^3}{2} + \frac{5\rho u k_{\rm B} T}{2\mu} + \frac{\rho u U}{\mu} + \frac{u B^2}{4\pi}\right] = \mathcal{B} \tag{2.45}$$

where

$$Bu = B_0 u_s$$

and where the subscript '0' denotes quantities in the preshock gas. Equivalently, we have [using equation (2.43)] that

$$\frac{\mathrm{d}}{\mathrm{d}z}\left(\frac{B}{\rho}\right) = 0 \tag{2.46}$$

when the magnetic field is frozen in the fluid.

The solution of equations (2.43), (2.44), (2.45) and (2.46) for the flow variables u, ρ, T and B, across the discontinuity and in the cooling flow, was considered by Field et al. [26]. If the molecular weight of the gas also varies, owing to reactions such as (2.41) above, equation (2.42) must also be included. We consider first the discontinuity, then the cooling flow.

2.3.1 The 'discontinuity' in a J*–type shock wave*

We have already noted that the width of the 'discontinuity' is determined by viscosity and thermal conduction, and hence by the distance scale for elastic scattering processes. Chemical reactions, including collisional dissociation (2.41), and collisional processes leading to the emission of radiation, and hence cooling, are all *in*elastic processes, for which the characteristic distance scales are larger, by at least an order of magnitude, than the corresponding elastic scattering processes. Thus, within the shock 'discontinuity', the source terms $\mathcal{N}$ and $\mathcal{B}$ in equations (2.42) and (2.45), respectively, can be taken equal to zero. Furthermore, the flux of internal energy is constant, as the populations of internal energy states do not change. In the context of the equation of energy conservation, the shock transition ('discontinuity') may be qualified as adiabatic, i.e. there is no exchange of energy with the shock's environment. Viscosity and thermal conduction are significant only within the shock transition, where the velocity and thermal gradients are large; these processes (viscosity and thermal conduction) are not included in the above equations, as they can be neglected on either side of the 'discontinuity'. Thus, relations can be obtained between the flow variables immediately downstream and upstream of the discontinuity. These equations – commonly referred to as the *Rankine–Hugoniot relations* – are

$$\rho_1 u_1 = \rho_0 u_s \tag{2.47}$$

$$\rho_1 u_1^2 + \frac{\rho_1 k_{\rm B} T_1}{\mu} + \frac{B_1^2}{8\pi} = \rho_0 u_s^2 + \frac{\rho_0 k_{\rm B} T_0}{\mu} + \frac{B_0^2}{8\pi} \tag{2.48}$$

$$\frac{\rho_1 u_1^3}{2} + \frac{5\rho_1 u_1 k_{\rm B} T_1}{2\mu} + \frac{u_1 B_1^2}{4\pi}$$

$$= \frac{\rho_0 u_s^3}{2} + \frac{5\rho_0 u_s k_{\rm B} T_0}{2\mu} + \frac{u_s B_0^2}{4\pi} \tag{2.49}$$

$$\frac{B_1}{\rho_1} = \frac{B_0}{\rho_0} \tag{2.50}$$

where the subscript '0' denotes the preshock gas, upstream of the discontinuity, '1' denotes the postshock gas, downstream of the discontinuity, and the molecular weight μ is constant. Equations (2.47) – (2.50) may be combined to yield a quadratic equation for the compression ratio, ρ_1/ρ_0, across the discontinuity:

$$2(2-\gamma)b\left(\frac{\rho_1}{\rho_0}\right)^2 + [(\gamma-1)M^2 + 2\gamma(1+b)]\frac{\rho_1}{\rho_0} - (\gamma+1)M^2 = 0 \tag{2.51}$$

In equation (2.51), M is the shock Mach number, the ratio of the shock speed, u_s, to the isothermal sound speed in the preshock gas, $(k_{\rm B}T_0/\mu)^{\frac{1}{2}}$; $b = B_0^2/(8\pi p_0)$ is the ratio of the magnetic pressure, $B_0^2/(8\pi)$, to the gas pressure, $p_0 = \rho_0 k_{\rm B} T_0/\mu$, in the preshock gas. The ratio of specific heats at constant pressure and volume, γ, should be taken equal to $5/3$, the value appropriate to a gas with only translational degrees of freedom; this is because the internal energy of molecules such as H_2 does not have time to adjust to the changes in the temperature and density across the shock discontinuity. This adjustment occurs in the cooling flow, where the equations for the populations of the rovibrational levels of H_2 should be solved in parallel with the hydrodynamic conservation equations, in order to follow correctly the variation in the internal energy, U.

In the absence of a magnetic field ($B_0 = 0 = B_1$), the compression ratio across the shock discontinuity is given by

$$\frac{\rho_1}{\rho_0} = \frac{p_0 + h^2 p_1}{p_1 + h^2 p_0} \tag{2.52}$$

where $h^2 = (\gamma+1)/(\gamma-1)$. The pressure ratio across the shock discontinuity, p_1/p_0, is related to the isothermal Mach number in the preshock gas by

$$M^2 = \frac{\gamma+1}{2}\frac{p_1}{p_0} + \frac{\gamma-1}{2} \tag{2.53}$$

The processes which determine the thickness of the shock transition – viscosity and thermal conduction – are irreversible and give rise to an increase in entropy across the shock front. It can be shown that, as a consequence, the condition $p_1 > p_0$ must apply; it follows from (2.52) that $\rho_1/\rho_0 > 1$. Thus, both the pressure and the density of the gas *increase* as the gas traverses the discontinuity. The quadratic equation (2.51) has two roots, in general, but only one of the solutions corresponds to a compression shock, in which $\rho_1/\rho_0 > 1$.

Equation (2.52) shows that, in the limit of $p_1 >> p_0$, $\rho_1/\rho_0 \to h^2 = 4$ for $\gamma = 5/3$. From equation (2.47), we see that, in this limit,

$$\frac{u_1}{u_s} = \frac{\rho_0}{\rho_1} = \frac{1}{4}$$

Thus, in the shock frame, the gas flows into the shock front at speed u_s and out at speed $u_s/4$. In an inertial frame in which the preshock gas is at rest, the gas is accelerated at the shock front to a speed $3u_s/4$.

The temperature rise at the discontinuity is given by

$$\frac{T_1}{T_0} = \frac{(p_1 + h^2 p_0)}{(p_0 + h^2 p_1)}\frac{p_1}{p_0} \tag{2.54}$$

Thus, in the limit of $p_1 >> p_0$, $T_1/T_0 \to (p_1/h^2 p_0)$. Unlike the compression ratio, the temperature ratio across the shock wave is unlimited.

The presence of a transverse magnetic field moderates the compression and the increase in temperature which occur at the shock front. As we have already seen, if the magnetic field is sufficiently strong, the discontinuity can be suppressed altogether, in C–type shock waves.

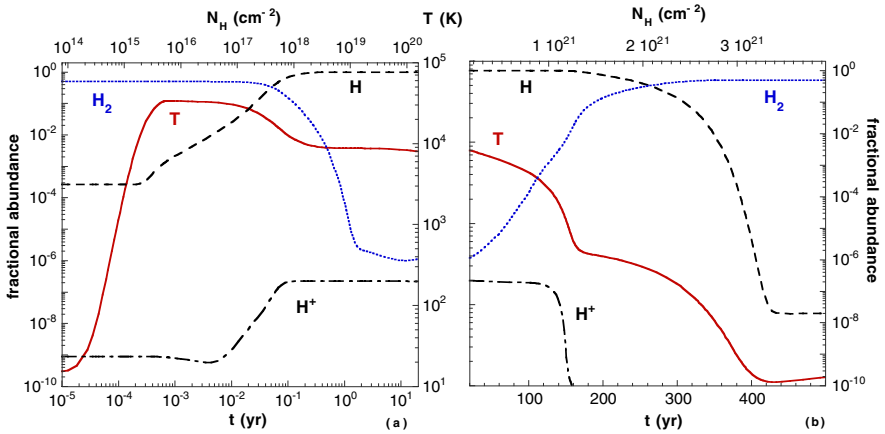

Fig. 2.1. The temperature profile computed for a J–type shock wave with a speed $u_s = 25$ km s^{-1}, propagating into gas of (preshock) density $n_{\rm H} = n({\rm H}) + n({\rm H_2}) + n({\rm H^+}) = 10^4$ cm^{-3}, in the absence of a magnetic field. The fractional abundances of H, H_2 and H^+ are also plotted. In the left hand panel, the abscissa (the flow time) is on a logarithmic scale.

2.3.2 The cooling flow of a J–type shock wave

If sufficiently hot, the compressed gas which flows out of a shock discontinuity is able to excite molecules, atoms and ions. These 'cooling' processes cause the temperature of the gas to fall whilst it continues to be compressed. By the time that the gas has cooled to its equilibrium (postshock) temperature, the total compression ratio, relative to the preshock gas, can be much greater than the maximum value of 4 at the shock discontinuity. The presence of a finite, transverse magnetic field limits the degree of compression of the gas.

The temperature profile computed for a J–type shock wave with a speed $u_s = 25$ km s^{-1}, propagating into gas of (preshock) density $n_{\rm H} = n({\rm H}) + n({\rm H_2}) + n({\rm H^+}) = 10^4$ cm^{-3}, in the absence of a magnetic field, is shown in Fig. 2.1. The independent variable in this Figure is the flow time,

$$t = \int \frac{1}{u}\, {\rm d}z$$

where z is the direction of flow and u is the flow speed, in the shock frame. In these calculations, the shock 'discontinuity' has a small but finite width, owing to artificial viscosity terms having been introduced into the conservation equations; these equations can then be integrated from the preshock through to the postshock, equilibrium gas.

The initial jump in temperature at the discontinuity is sufficient for collisional dissociation to take place, as may be seen from Fig. 2.1, where the abundances of H, H_2 and H^+, relative to $n_{\rm H}$, are plotted. In fact, molecular hydrogen is rapidly collisionally dissociated in the hot gas behind the 'discontinuity', on a flow timescale of the order of 1 yr. The main coolants of the gas are then atoms and ions, notably atomic oxygen, through its fine structure transitions at 63 and 147 μm (see Chapter

6). In the cooling flow, H_2 reforms (on grains), and the associated heating of the gas gives rise to the 'knee' in the temperature profile, apparent in the right hand panel of Fig. 2.1. Finally, after approximately 500 yr, the kinetic temperature reaches its postshock equilibrium value, of the order of 10 K. The total compression ratio in this case approaches 10^4: there is no magnetic field to moderate the compression of the gas.

Referring to equation (2.45), we see that, in the absence of a magnetic field, contributions to the energy flux arise from: (i) the kinetic energy of the flow; (ii) the thermal energy of the gas; (iii) the internal energy of the gas; (iv) radiative losses (incorporated in $\mathcal{B}$). In the preshock gas, (i) dominates. Immediately behind the 'discontinuity', (ii) is the major term, with some contribution from (iii) at the beginning of the cooling flow. Finally, radiative losses take over and the gas cools to its postshock, equilibrium state.

2.3.3 C–*type shock waves*

The interaction of the gas and the grains with the magnetic field is crucially important to the development of C–type shock waves. The field couples directly to the charged fluid and thence to the neutral fluid, which contains most of the mass, via collision processes (cf. Section 2.2 above). The strength of the coupling between the charged and neutral fluids depends on the degree of ionization of the gas and hence on the rates of chemical reactions which modify the degree of ionization within the shock wave. The coupling between the charged and neutral fluids also depends on the fraction of the grains which is (principally negatively) charged. Although the *number density* of the grains is much smaller than that of the gaseous ions, their *mass density* is, in dark clouds, much larger.

By way of illustration of the importance of chemical reactions in this context, Fig. 2.2 compares the fractional ionization of the gas and the thermal profiles computed for a C–type shock wave of speed $u_s = 10$ km s^{-1} which propagates into gas of preshock density $n_{\rm H} = 10^3$ cm^{-3} and in which the tranverse magnetic field strength is $B_0 = 25$ μG; in one calculation, chemical reactions were neglected, and, in the other, they were included. As may be seen from this Figure, the degree of ionization is modified considerably by the chemistry, both within the shock wave and in the postshock, equilibrium gas. Endothermic reactions between atomic ions and H_2 are activated by the ion–neutral drift speed within the shock wave, and the molecular ions which are produced are able to recombine rapidly with electrons. Thus, the fractional ionization *falls* within the shock wave when the chemistry is included. On the other hand, when the chemistry is neglected, the fractional ionization increases, owing to the differential compression of the ions, before falling back to its equilibrium value in the postshock gas. To a lower degree of ionization corresponds a more extended shock wave, in which the neutral fluid has a lower maximum temperature.

Fig. 2.2 also shows that the time of flow through a C–type shock wave, from the preshock to the postshock, equilibrium gas, is of the order of 10^5 yr; this is very much greater than in a J–type shock wave of comparable speed. As the time to reach steady–state cannot be less than the time of flow through the shock wave, it follows that C–type shock waves do not attain steady–state under conditions, such as those in jets, in which the dynamical timescales are much less than 10^5 yr.

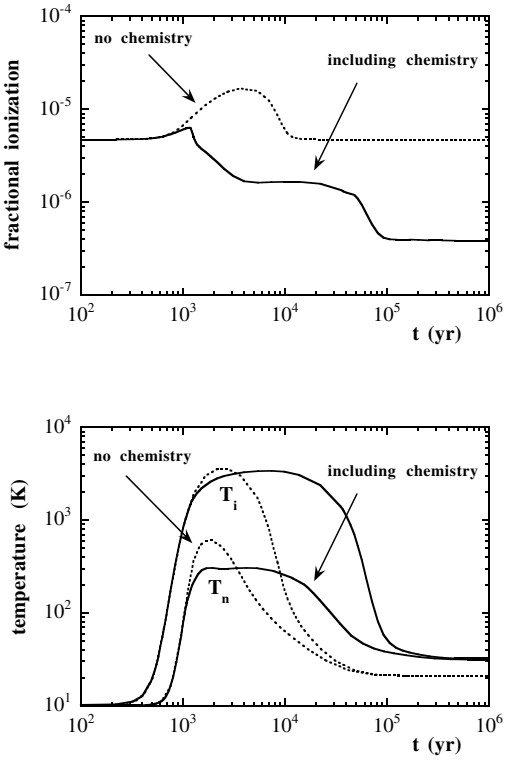

Fig. 2.2. The fractional ionization of the gas and the thermal profiles in a C–type shock wave of speed $u_s = 10$ km s^{-1}, which propagates into gas of preshock density $n_{\rm H} = 10^3$ cm^{-3} in which the transverse magnetic field strength $B_0 = 25$ μG.

In order to determine rigorously the structure of shock waves in their evolution to a steady state, a time–dependent MHD code is necessary. Such codes have been developed, but they are still restricted in the range and complexity of the physico–chemical processes which can be incorporated. An alternative approach, which provides an approximation to the time–dependent shock structure that is acceptable in the context of many applications, will be presented below.

When there is a disturbance which propagates at supersonic speed in a medium, a shock wave can be produced. Stellar winds, jets, turbulence, and collisions between interstellar clouds, for example, are all susceptible to generating shock waves. The concept of 'steady state' is relevant only if the mechanism responsible for producing the shock wave endures for at least the time required for the shock wave to attain its equilibrium state. Evanescent phenomena must, by their nature, be studied by means of an explicitly time–dependent model. The energy source which creates and maintains a shock wave may be compared with the 'piston' that can be used to generate shock waves in the laboratory. Let us denote the speed of propagation of the piston by $u_{\rm p}$. We shall assume that $u_{\rm p}$ is constant and show, from considerations of the continuity of the flow, that the shock front propagates at a speed, $u_{\rm s}$, which somewhat exceeds $u_{\rm p}$.

As is customary, we apply the equation of continuity in the frame of the shock wave, i.e. the frame in which the shock front is at rest; this is achieved by subtracting the shock velocity, $\mathbf{u}_\mathrm{s}$, from velocities in an inertial frame, usually taken to be the frame of the preshock gas. Referring to equation (2.47), we see that

$$u_1 = \frac{u_\mathrm{s}}{(\rho_1/\rho_0)} \tag{2.55}$$

where ρ_0, ρ_1 denote the preshock and postshock gas density, respectively, and u_1 is the postshock flow speed; the ratio (ρ_1/ρ_0) is the compression factor. In the inertial frame, the preshock gas is at rest and the postshock gas flows at speed

$$u_\mathrm{s} - \frac{u_\mathrm{s}}{(\rho_1/\rho_0)}$$

in the direction of propagation of the shock front. At the surface of the piston, the gas is moving with the speed of the piston, u_p, and hence

$$u_\mathrm{p} = u_\mathrm{s}\left[1 - \frac{1}{(\rho_\mathrm{p}/\rho_0)}\right] \tag{2.56}$$

where ρ_p is the value of ρ_1 the surface of the piston. It follows from (2.56) that $u_\mathrm{s} > u_\mathrm{p}$.

If the shock is initially J–type, the compression factor at the discontinuity is $(\rho_1/\rho_0) = 4$, in the limit of large Mach numbers. Then, $u_\mathrm{s} = 4u_\mathrm{p}/3$, and the shock discontinuity moves away from the piston, with which it was initially in contact. In the cooling flow which develops between the discontinuity and the piston, the gas is compressed further and the speed of the shock front decreases towards that of the piston (which is assumed constant). By the time that the compression factor at the surface of the piston has become large $[(\rho_\mathrm{p}/\rho_0) >> 1]$, the piston and the shock front are travelling at the same speed. From equation (2.56), it may be seen that the speed with which the shock front moves away from the piston, $u_\mathrm{s} - u_\mathrm{p} = u_\mathrm{s}/(\rho_\mathrm{p}/\rho_0)$, is also the speed of fluid flow (in the reference frame of the shock wave) at the surface of the piston.

If the transverse magnetic field strength is sufficiently large, a magnetic precursor develops upstream of the shock discontinuity and preheats the gas. As a consequence, the sound speed in the gas immediately upstream of the discontinuity increases and the Mach number falls, i.e. the shock discontinuity weakens. By the time that steady–state is attained, the discontinuity may have disappeared altogether, in which case the structure has become pure C–type; this evolution is illustrated in Fig. 2.3. This Figure shows also the shock front gradually separating from the 'piston' as time progresses; the speed of the shock front, relative to the piston, decreases as the compression factor increases.

The evolution of the shock wave, from initially pure J–type, to J–type with a magnetic precursor, seen in Fig. 2.3, to finally C–type, may be simulated by introducing a discontinuity in the flow at a point in the steady–state profile which is located increasingly downstream as time advances. The time is given by the time of flow of a fluid particle through the precursor to the discontinuity,

$$t = \int \frac{1}{u}\,\mathrm{d}z$$

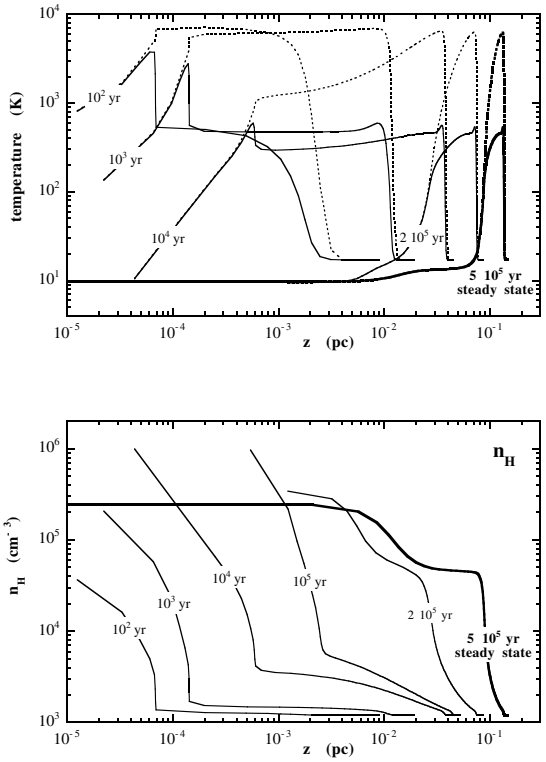

Fig. 2.3. Temperature and density profiles as functions of position and time for a shock wave of speed $u_s = 10$ km s^{-1}, propagating into gas of density $n_{\rm H} = 10^3$ cm^{-3} in which the transverse magnetic field strength $B_0 = 25$ μG. The shock wave advances from left to right until a stationary state is finally attained. The origin of the position coordinate, z, is at the 'piston'.

The steady–state structure of the shock wave 'unfolds' as time progresses. Comparisons with the results of explicitly time–dependent MHD calculations ([32], [33]) have shown that the evolution of the shock wave is satisfactorily described by means of the approximation outlined above.

2.4 Shock waves in dark clouds

The characteristics and spectroscopic signatures of J–type shock waves propagating in molecular media have been studied for many years. In the cooling flow behind the discontinuity, molecules, atoms and ions can be collisionally excited in the shock–heated gas. Rovibrational molecular transitions, fine structure and other 'forbidden' atomic and ionic transitions are emitted and, when detected, provide diagnostic information on the medium.

The physical state and chemical composition of the cooling flow depend on the shock speed, the transverse magnetic field strength in, and the density of, the preshock gas. With increasing shock speed, $u_{\rm s}$, the maximum postshock temperature increases to values (of the order of 10^3 K) at which the collisional excitation of

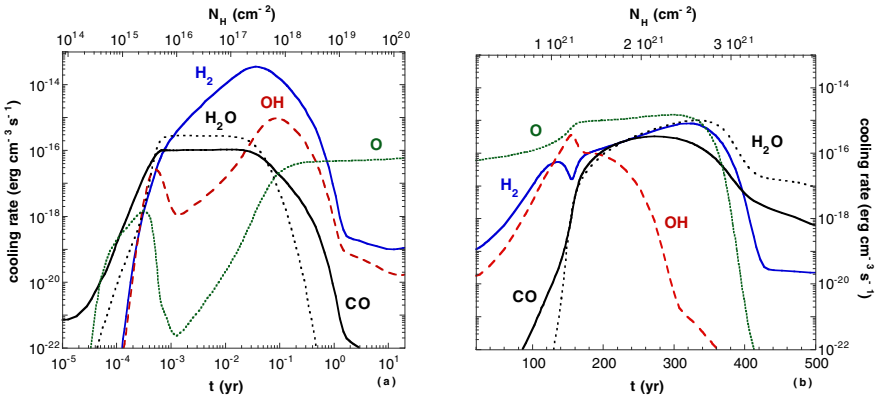

Fig. 2.4. The rates of cooling by the principal coolants for a J–type shock wave with a speed $u_s = 25$ km s^{-1}, propagating into gas of (preshock) density $n_{\rm H} = n({\rm H}) + n({\rm H_2}) + n({\rm H^+}) = 10^4$ cm^{-3}, in the absence of a magnetic field. In the left hand panel, the abscissa (the flow time) is on a logarithmic scale.

molecular hydrogen begins to be significant. As $u_{\rm s}$ increases further and the temperature reaches approximately 10^4 K, electronic excitation of atomic hydrogen occurs and, ultimately, H is collisionally ionized. The ultraviolet radiation produced by the radiative decay of the electronically excited states of H becomes sufficiently intense to pre–ionize the gas upstream of the shock discontinuity; the shock wave is then said to have a *radiative precursor*. If the transverse magnetic field is weak or absent, shock speeds $u_{\rm s} \approx 25$ km s^{-1} are sufficient to cause almost complete dissociation of H_2 immediately downstream of the discontinuity.

In Fig. 2.4 are illustrated the contributions of various atomic and molecular species to the cooling of a J–type shock wave of speed $u_{\rm s} = 25$ km s^{-1}, preshock density $n_{\rm H} = 10^4$ cm^{-3} and transverse magnetic field strength $B_0 = 0$. The collisional dissociation of molecular hydrogen releases atomic hydrogen into the hot gas, leading to the destruction of other molecular species. For example, the reactions

$$H_2O + H \rightarrow OH + H_2$$

and

$$OH + H \rightarrow O + H_2$$

return oxygen to atomic form. Through its fine structure transitions at 63 μm and 147 μm, O then becomes the principal coolant of the gas. As the gas cools down, first H_2 reforms, and then other molecules, such as H_2O and CO. The time required for the medium to reach its postshock equilibrium temperature is approximately 500 yr. Thus, in dynamically young objects, even J–type shock waves may not have had sufficient time to reach steady state.

As the shock speed increases beyond $u_{\rm s} = 25$ km s^{-1}, the extent of the cooling flow (and the time required for the gas to attain its postshock equilibrium temperature) begins to *decrease*. This reversal occurs because the degree of ionization of atomic hydrogen, and consequently the fractional electron abundance, increase rapidly with

u_s above approximately 25 km s^{-1}. Cooling of the medium owing to electron collisional excitation of atomic hydrogen, principally the Ly α transition, then becomes important.

The populations of the rovibrational levels of H_2 do not respond instantaneously to the changes in temperature and density which occur at and behind the shock discontinuity. Indeed, as we have already seen, excitation of the internal degrees of freedom of H_2 is insignificant within the shock 'discontinuity', where the flow variables change adiabatically. In the cooling flow, immediately behind the discontinuity, the level populations respond to changes in the temperature and density on a timescale which, by definition, is comparable with the local cooling time (on which the temperature changes significantly), as H_2 is the principal coolant of the gas. Under these conditions, it is essential to integrate the differential equations governing the H_2 level populations in parallel with the dynamical equations and the chemical rate equations.

In the presence of a transverse magnetic field of sufficient strength, an initially J–type shock wave develops a magnetic precursor and can ultimately become C–type. In order for a precursor to develop, the magnetosonic speed, c_m [equation (2.17)], must exceed the shock speed, u_s. As the physical conditions in the preshock gas determine the value of the magnetosonic speed, the requirement that $u_s < c_m$ sets a upper limit on the speed of shock waves which can become C–type.

The physical conditions in the preshock gas, notably the degree of ionization, depend on the rate of cosmic ray ionization of hydrogen, ζ. Most of the positive charge is associated with atomic and molecular ions in the gas. However, contributions to the negative charge arise not only from the free electrons but also from negatively charged grains and, possibly, from anions of polycyclic aromatic hydrocarbons (PAH). The distribution of the negative charge amongst free electrons, grains and PAH depends on the fractional abundance of the PAH molecules and on the rates of electron attachment and detachment reactions, as well as the rates of recombination of positive ions with electrons on the surfaces of negatively charged grains; all these parameters are subject to significant uncertainties.

In Fig. 2.5 are plotted the values of the magnetosonic speed computed for a range of densities of the preshock gas and of fractional abundances of PAH molecules; the cosmic ray ionization rate is $\zeta = 1 \times 10^{-17}$ s^{-1} and the transverse magnetic field strength $B_0 = [n_H]^{0.5}$, where n_H is in units of cm^{-3} and B_0 is in μG. The density dependence of B_0 is such as to ensure that the magnetic energy density in the preshock gas scales in proportion to the thermal energy density, at a given temperature.

Also plotted in Fig. 2.5 is the critical shock speed at which the degree of collisional dissociation of H_2, the principal coolant, becomes sufficient for a thermal runaway to occur. There results a sonic point in the flow (owing to the rapidly rising temperature and hence sound speed), and the shock becomes J–type. It may be seen from Fig. 2.5 that, for $n_{PAH}/n_H = 10^{-6}$ and $n_H > 10^4$ cm^{-3}, the upper limit to the possible speed of a C–type shock wave is determined by the collisional dissociation of H_2, whereas, for $n_H < 10^4$ cm^{-3}, it is determined by the magnetosonic speed in the preshock gas. The limit imposed by the magnetosonic speed becomes more stringent for $n_{PAH}/n_H < 10^{-6}$. Although still uncertain, the fraction of carbon which is believed

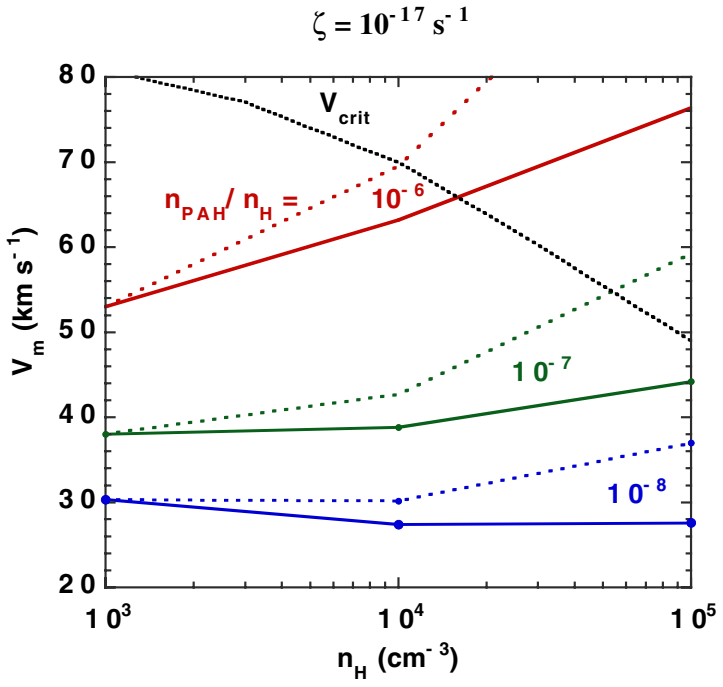

Fig. 2.5. The magnetosonic speed in preshock gas of density $10^3 \leq n_{\rm H} \leq 10^5$ cm^{-3} and fractional abundance of PAH $10^{-8} \leq n_{\rm PAH}/n_{\rm H} \leq 10^{-6}$; the cosmic ray ionization rate is $\zeta = 1 \times 10^{-17}$ s^{-1} and the transverse magnetic field strength B_0 μG $= [n_{\rm H}]^{0.5}$, where $n_{\rm H}$ is in units of cm^{-3}.

to exist in 'very small grains' sets an upper limit to the fractional abundance of the PAH, namely $n_{\rm PAH}/n_{\rm H} \lesssim 10^{-6}$.

The steady–state thermal, velocity and density profiles of the neutral and charged fluids for an illustrative C–type shock wave are shown in Fig. 2.6. These profiles display a number of characteristics of C–type shock structure: the initially rapid decoupling of the velocity of the charged fluid from that of the neutrals, followed by their recoupling on a timescale of the order of 10^3 yr for the model shown; the initial increase in the fractional ionization, owing to the differential compression of the charged fluid, followed by a decrease (by approximately 3 orders of magnitude in the model shown) to its postshock value; the decoupling of the temperatures of the charged fluids from the temperature of the neutrals and, over a more restricted time range, the decoupling of the temperature of the ions from that of the electrons. The electron temperature lies between the temperatures of the ions and the neutrals: the much greater abundance of the neutrals compensates for the stronger thermal coupling of the electrons to the positive ions (which is mediated by the attractive Coulomb force). Owing to the differential compression of the charged fluid and the initial rise in $T_{\rm e}$, the rate of electron attachment to grains is sufficient to ensure that the grains are predominantly negatively charged within the shock wave. The rate equations which determine the grain charge must be solved in parallel with the

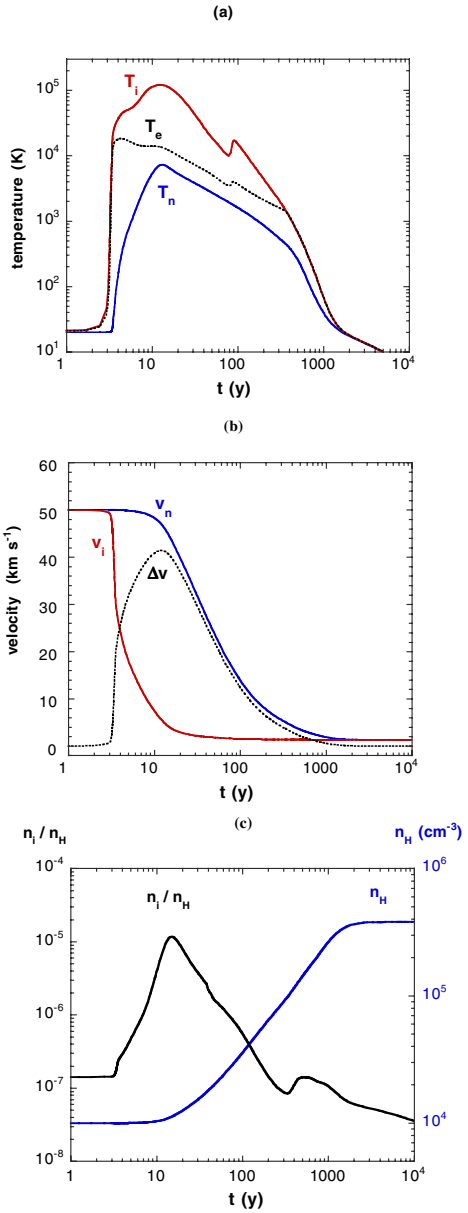

Fig. 2.6. The steady–state profiles of (a) temperature, (b) velocity ($\Delta v = v_{\rm n} - v_{\rm i}$, and (c) density of the neutral and charged fluids, for an illustrative C–type shock wave of speed $v_{\rm s} = 50$ km s^{-1}, preshock density $n_{\rm H} = 10^4$ cm^{-3}, and transverse magnetic field strength $B_0 = 100$ μG.

equations which describe the dynamical structure of the shock wave, because the chemistry and the dynamics interact strongly.

2.5 Shock waves in diffuse clouds

The interstellar background ultraviolet radiation field permeates diffuse clouds and ionizes species with ionization potentials less than that of atomic hydrogen. Consequently, in diffuse gas, the most abundant ion is C^+. It has already been mentioned that endothermic reactions, such as

$$C^+ + H_2 \rightarrow CH^+ + H - 4640 \text{ K}$$

can become significant in shocked gas; this is true also of reactions such as

$$O + H_2 \rightarrow OH + H$$

which is endothermic and has a barrier, and of

$$OH + H_2 \rightarrow H_2O + H$$

which has a barrier. In a medium which is rich in molecular hydrogen, the reaction of C^+ with H_2 is followed rapidly by the exothermic hydrogenation reactions

$$CH^+ + H_2 \rightarrow CH_2^+ + H$$

and

$$CH_2^+ + H_2 \rightarrow CH_3^+ + H$$

beyond which the sequence proceeds much more slowly, either by radiative association

$$CH_3^+ + H_2 \rightarrow CH_5^+ + h\nu$$

or by the strongly endothermic reaction

$$CH_3^+ + H_2 \rightarrow CH_4^+ + H - 32500 \text{ K}$$

All of the hydrocarbon ions which are formed undergo dissociative recombination reactions with electrons, such as

$$CH_n^+ + e^- \rightarrow CH_{n-1} + H$$

$$CH_n^+ + e^- \rightarrow CH_{n-2} + H_2$$

$$CH_n^+ + e^- \rightarrow CH_{n-2} + H + H$$

the net effect being the neutralization of C^+ ions in the gas.

The key reaction in the above hydrogenation cycle is $C^+(H_2, H)CH^+$, which is endothermic by 4640 K. ambipolar diffusion in shock waves will drive this reaction once the relative kinetic energy of the ions and the neutrals is comparable with the endothermicity, i.e. once $\mu_{in}(u_i - u_n)^2/(2k_B) \approx 4640$ K, where $\mu_{in} = \mu_i\mu_n/(\mu_i + \mu_n)$ is the reduced mass of the C^+–H_2 pair. This relation implies that the relative drift speed,$(u_i - u_n)$, should be at least 6 or 7 km s^{-1}. Such speeds are readily attained in shock waves with speeds $u_s \gtrsim 10$ km s^{-1} in which the magnetic field strength in the preshock gas, B_0, is a few μG.

Photoreactions prevent ambipolar diffusion leading to the complete neutralization of the C^+ component of the ionized gas. The CH_n molecules which are the products of the above cycle are photodissociated

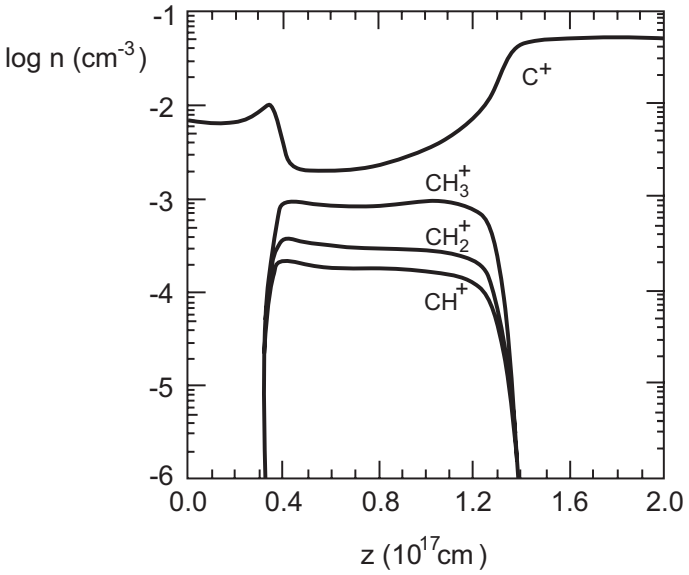

Fig. 2.7. The densities of C–bearing ions through a C–type shock wave of speed 12 km s^{-1}, propagating into a diffuse interstellar cloud in which the preshock density $n_{\rm H} = 20$ cm^{-3} and the transverse magnetic field strength $B_0 = 5$ μG.

$$\mathrm{CH}_n + h\nu \rightarrow \mathrm{CH}_{n-1} + \mathrm{H}$$

$$\mathrm{CH}_n + h\nu \rightarrow \mathrm{CH}_{n-2} + \mathrm{H}_2$$

and the atomic carbon which is produced is then photoionized

$$\mathrm{C} + h\nu \rightarrow \mathrm{C}^+ + \mathrm{e}^-$$

As a result of these reactions, C^+ ions are restored to the gas over a distance scale which is comparable with the MHD shock width. Thus, the C^+ density in such a shock wave first rises owing to the compression of the ionized gas, then falls as a result of ion–molecule reactions and dissociative recombination, and finally rises again as photoreactions take over. This behaviour is illustrated in Fig. 2.7. The pre– and post–shock values of the density of C^+ ions are determined by the equilibrium between the rate of photoionization of C and the reverse process, namely, radiative recombination of C^+ with electrons.

It has already been mentioned that, in shock–heated gas, the chemistry of oxygen is initiated by the reaction O(H_2, H)OH which has a barrier of 2980 K (which is larger than the endothermicity of approximately 960 K). The subsequent reaction, OH(H_2, H)H_2O, has a smaller barrier of 1490 K. Photodissociation of H_2O and OH eventually returns O to the gas. Reactions of C^+ and CH_n^+ with O and OH_n lead to the formation of CO^+ and $\mathrm{H}_n\mathrm{CO}^+$, which recombine dissociatively with electrons. The molecules which are so produced are ultimately photodissociated into C and O. The end result is the restoration of oxygen to its atomic form in the postshock gas. However, the facility with which water is produced in shock waves, through the reactions O(H_2, H)OH and OH(H_2, H)H_2O, results in fractional abundances of

H_2O which exceed that observed in shocked molecular gas associated with IC443 (a supernova remnant) by the SWAS satellite [39]. Thus, although the transformation of atomic oxygen into water in shock waves was believed to be well understood, the models failed their first observational test. Other surprises of this type undoubtedly await us.